Effects of photogenerated carrier scattering on the decay process of coherent longitudinal optical phonons in an undoped GaAs/n-type GaAs epitaxial structure investigated by terahertz time-domain spectroscopy

Hideo Takeuchi, Takahiro Sumioka, Masaaki Nakayama

Effects of photogenerated carrier scattering on the decay process of coherent longitudinal optical phonons in an undoped GaAs/n-type GaAs epitaxial structure investigated by terahertz time-domain spectroscopy

Hideo Takeuchi, Takahiro Sumioka, and Masaaki Nakayama

Citation: Journal of Vacuum Science & Technology A: Vacuum, Surfaces, and Films **35**, 04D104 (2017); doi: 10.1116/1.4983637

View online: http://dx.doi.org/10.1116/1.4983637

View Table of Contents: http://avs.scitation.org/toc/jva/35/4

Published by the American Vacuum Society

Effects of photogenerated carrier scattering on the decay process of coherent longitudinal optical phonons in an undoped GaAs/*n*-type GaAs epitaxial structure investigated by terahertz time-domain spectroscopy

Hideo Takeuchi,[a] Takahiro Sumioka, and Masaaki Nakayama
Department of Applied Physics, Graduate School of Engineering, Osaka City University, 3-3-138 Sugimoto, Sumiyoshi, Osaka 558-8585, Japan

(Received 14 March 2017; accepted 1 May 2017; published 23 May 2017)

The authors investigated the scattering effect of photogenerated carriers on the decay of the coherent longitudinal optical (LO) phonons in an undoped GaAs/*n*-type GaAs epitaxial structure using a terahertz time-domain spectroscopic technique. The terahertz wave from the coherent LO phonon was observed together with those emitted both by the ultrafast photocurrent and by the coherent LO-phonon-plasmon coupled (LOPC) mode. The simultaneous observation of the coherent LO phonon and coherent LOPC mode originates from the fact that the photogenerated carrier density laterally distributes around the surface of the undoped GaAs layer owing the Gaussian profile of the pump beam. The authors found that the terahertz wave from the coherent LO phonon lives up to 5.0 ps, whereas those from the coherent LOPC mode and ultrafast photocurrent disappear within 1.0 ps. The decay time of the coherent LO phonon monotonically decreases with an increase in the pump power. This finding indicates that the dephasing of the terahertz wave from the coherent LO phonon is dominated by the photogenerated carrier scattering in the time range shorter than 1.0 ps in which photogenerated carriers remain. © *2017 American Vacuum Society*.
[http://dx.doi.org/10.1116/1.4983637]

I. INTRODUCTION

Illumination of femtosecond-laser pulses on semiconductor surfaces generates temporal terahertz electromagnetic waves. This phenomenon has been attracting much attention in the research field of semiconductor surfaces because it provides time-domain information on the dynamical phenomena around the surface.[1] It is well known that an ultrafast current, which is produced by photogenerated carriers, emits a terahertz wave.[2] The terahertz wave originating from the ultrafast photocurrent is usually observed as a bipolar pulse in the time-domain signal. The electric field of the terahertz wave $\mathbf{E}_{\mathrm{THz}}$ is proportional to time derivative of the ultrafast photocurrent $\mathbf{J}$: $\mathbf{E}_{\mathrm{THz}} \propto \partial\mathbf{J}/\partial t$. The direction of the ultrafast photocurrent reflects those of the surface electric field and band bending. Utilizing the characteristics of the bipolar pulse, we clarified that the direction of the surface electric field is inversed by incorporation of dilute nitrogen to GaAs from the observation of the polarity reversal of the bipolar pulse.[3] Recently, Sano *et al*. reported that, based on a change in the shape of the bipolar pulse, the surface depletion layer of a graphene-coated InP substrate is sensitively changed by the presence of localized electric dipoles induced by adsorbed oxygen.[4] A similar phenomenon was observed in an InP substrate covered with a WS_2 nanosheet.[5] We note that the illumination of the femtosecond-laser pulses also generates the terahertz waves from coherent longitudinal optical (LO) phonons. The coherent LO phonon is regarded as a dynamical longitudinal polarization $\mathbf{P}_{\mathrm{LO}}$, so that it emits the terahertz wave with an electric field of $\mathbf{E}_{\mathrm{THz,LO}} \propto \partial^2\mathbf{P}_{\mathrm{LO}}/\partial t^2$. The terahertz-wave emission from the coherent LO phonon is triggered by the instantaneous screening effect of the ultrafast photocurrent on the surface electric field.[6–8] The instantaneous screening releases the initial polarization (initial amplitude) of the coherent LO phonon induced by the surface electric field, which leads to the polarization oscillation of the coherent LO phonon. The polarization oscillation produces the terahertz-wave emission from the coherent LO phonon. The emission mechanism described above indicates that the terahertz wave from the coherent LO phonon connects with the surface electric field; therefore, the coherent LO phonon provides the information on the dynamics around the surface. We note that the ensemble of the photogenerated carriers forms the plasmon oscillating longitudinally. According to the well-known coupled vibration theory, the coherent LO phonon couples with the plasmon and forms the LO-phonon-plasmon coupled (LOPC) mode.[9] The coherent LO phonon and coherent LOPC mode were intensively investigated with the use of terahertz time-domain spectroscopy[7,8,10–16] and ultrafast optical pump-probe spectroscopy.[6,7,17–25] We, here, point out the fact that the interaction between the coherent LO phonon and photogenerated carriers is not limited within the formation time of the coherent LOPC mode. The earlier works did not reveal the scattering effect of photogenerated carriers on the coherent LO phonon.

In the present paper, using terahertz time-domain spectroscopy, we demonstrate that the photogenerated carriers actually influence the dephasing of the coherent LO phonon. We used a sample composed of an undoped GaAs top layer and a heavily doped *n*-type GaAs bottom layer, which is refereed as the undoped GaAs/*n*-type GaAs epitaxial structure.

[a]Electronic mail: takeuchi@a-phys.eng.osaka-cu.ac.jp

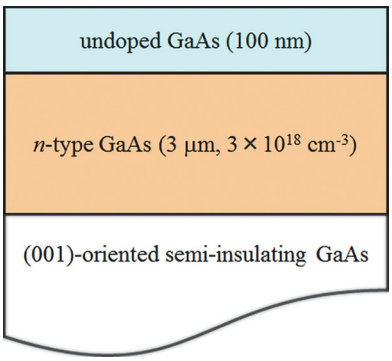

FIG. 1. (Color online) Schematic structure of the present sample. The values in the parenthesis denote the thicknesses and doping concentration of the *n*-type and undoped GaAs layers.

In the present sample, the undoped GaAs layer has a relatively large and uniform built-in electric field owing to the surface Fermi level pinning.[26] This is advantageous to observe the intense terahertz waves emitted by the coherent LO phonon and LOPC mode in addition to that by the ultrafast photocurrent. Accordingly, the present sample has good suitability in investigating the scattering effect of the photogenerated carriers on the coherent LO phonon. We observed that the coherent LO phonon and coherent LOPC mode emit the terahertz wave. We found that the coherent LOPC mode disappears within 1.0 ps, while only the coherent LO phonon lives up to 5.0 ps. We revealed that the terahertz-wave decay time of the coherent LO phonon shortens as the pump laser power is increased. We discuss the decrease of the decay time in terms of the scattering effect of instantaneously photogenerated carriers.

II. SAMPLES AND EXPERIMENTAL PROCEDURE

The sample used in the present work was an undoped GaAs/*n*-type epitaxial structures grown on a (001)-oriented semi-insulating GaAs substrate by metal organic vapor phase epitaxy. Figure 1 shows the schematic sample structure. The thicknesses of the undoped and *n*-type layers were 100 nm and 3.0 μm, respectively, and the doping concentration was $3 \times 10^{18}\,\mathrm{cm}^{-3}$ in the *n*-type layer. The electric field strength built in the undoped GaAs layer was estimated to be 49 kV/cm (Ref. 16) from the analysis of the Franz-Keldysh oscillation[27] observed in a photoreflectance spectrum. We notice that the degenerate *n*-type GaAs layer hardly has the depletion region with a finite electric field owing to the too short screening length. Consequently, the initial polarization (initial amplitude) of the LO phonon, which also causes that of the LOPC mode, is negligible in the *n*-type layer.[16] Figure 2 shows the schematic experimental setup of the present terahertz time-domain spectroscopic measurement, which is a typical system based on an optical gating method with the use of a photoconductive dipole antenna formed on a low-temperature-grown GaAs epitaxial layer for detecting the terahertz wave emitted from the sample. The gap of the dipole antenna was 6 μm. The pump and probe light source was a Ti:sapphire laser with pulse duration of 50 fs and a repetition rate of 90 MHz, and the photon energy was 1.55 eV. In the present measurement, the time delay of the probe light was generated with a stepper equipped with a retroreflector. The time-delay range was from −2.0 to 6.0 ps. The pump light, the power of which was varied with a neutral density filter, was chopped at a frequency of 2.0 kHz and focused on the sample surface. The angle of the pump-light incidence was 45°. The spot diameter of the pump light, which had a Gaussian profile, was about 100 μm on the sample surface. Using a pair of parabolic mirrors, the terahertz wave emitted from the sample was focused on the photoconductive dipole antenna. The photocurrent obtained from the photoconductive dipole antenna was amplified by a current–voltage converter and was detected with a lock-in amplifier. All the measurements were carried out at room temperature. We used a purge of dry nitrogen gas and kept the humidity being about 5% to suppress the noise arising from the water-vapor absorption.

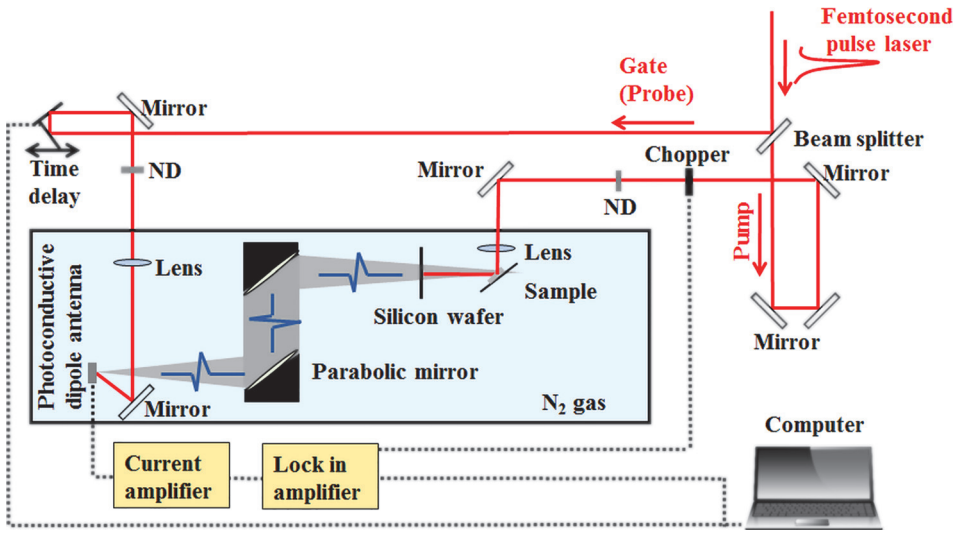

FIG. 2. (Color online) Schematic experimental setup of the present terahertz time-domain measurement.

III. EXPERIMENTAL RESULTS AND DISCUSSION

Figure 3 shows the terahertz time-domain signals from the present sample at various pump powers. The bipolar pulse, which results from the ultrafast photocurrent, appears at the time delay of 0 ps. The bipolar pulse is followed by the oscillation pattern with the period of 114 fs. The oscillation is clearly observed up to 5.0 ps. Since the oscillation period corresponds to the LO phonon frequency of GaAs (8.79 THz), we assign the origin of the oscillation pattern to the terahertz wave from the coherent LO phonon in the undoped GaAs layer. We note that the terahertz-wave decay time of the coherent LO phonon decreases as the pump power is increased, which is the main topic in the present paper and will be discussed later. In addition, the profile of the waveform in the time-delay range from 0 and to 0.4 ps is modified by an increase in the pump power; namely, certain components, which are related to the photogenerated carrier density, exist in this time-delay range. For clarifying the components of the time-domain signals, we performed the Fourier transform, the results of which are shown in Fig. 4. The dashed curves are obtained from the line-shape analysis of the Fourier power spectra, assuming four Gaussian-shape bands from the phenomenological viewpoint. The sharp band at the frequency of 8.8 THz originates from the coherent LO phonon. It is noted that the frequency range in a typical terahertz time-domain spectroscopic system is usually up to ~5 THz; however, that in the present system is up to ~10 THz as shown by Fig. 4. This wide frequency range may be due to high sensitivity of the photoconductive dipole antenna used in the present experiment. The broad band peaking at 2.2 THz is assigned to the bipolar pulse in the terahertz time-domain wave. The peak frequencies of the two bands due to the coherent LO phonon and bipolar pulse are independent of the pump power. The peak frequencies of other two bands, which are labeled by L_- and L_+, are pump-power dependent. In the earlier work, we revealed that the L_- and L_+ bands originate from the lower and upper branches of the LOPC mode formed in the undoped GaAs layer.[16] The

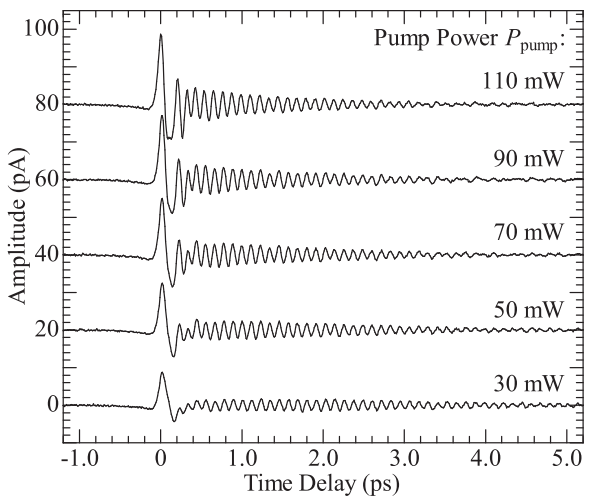

FIG. 3. Time-domain terahertz waveforms of the present sample at various pump powers.

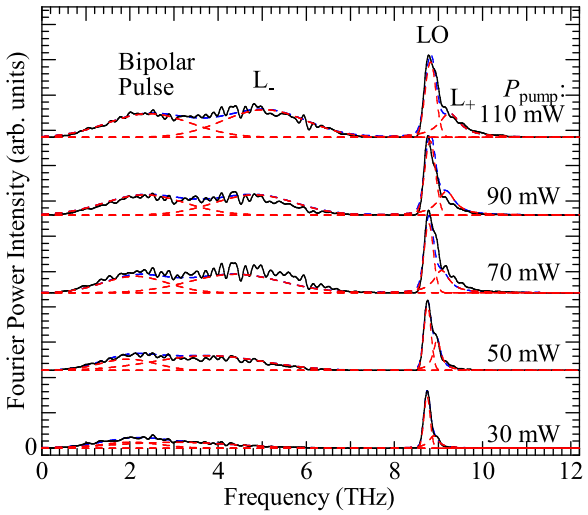

FIG. 4. (Color online) Fourier power spectra of the terahertz-wave signals shown in Fig. 3.

coherent LO phonon and coherent LOPC bands are simultaneously observed in the present experiment. As mentioned in Sec. II, the pump light has a Gaussian beam profile, which results in the lateral distribution of the photogenerated carrier density in the undoped GaAs layer. Around the center of the beam spot on the sample surface, the coupling between the coherent LO phonon and plasmon becomes considerable with an increase in photogenerated carrier density. As a result, the coherent LOPC mode is formed and emits the terahertz wave. In contrast, around the edge of the beam spot, the photogenerated carrier density is relatively low; therefore, the formation of the LOPC mode is negligible. Consequently, the coherent LO phonon emits the terahertz wave. Taking account of the fact that the terahertz wave from the coherent LO phonon is emitted from the whole of the edge regions in the excitation spot, we consider that the observed terahertz wave from the coherent LO phonon results from an average of the dynamical polarization created by the ensemble of coherent LO phonons.

Next, we focus our attention to the decay of the observed terahertz waves. Figure 5 shows the time-partitioning Fourier transform spectra $I(\omega)$ of the time-domain waveform $A(t)$ at 110 mW. The spectra of $I(\omega)$ were obtained with the use of the following equation:[19,20]

$$I(\omega) = \left| \int_{\tau}^{6\,\mathrm{ps}} A(t) \exp(-i\omega t) dt \right|^2 . \quad (1)$$

Here, τ is the time delay determining the time window of the time-partitioning Fourier transform. The ordinal Fourier power spectrum, which is obtained without applying the time-partitioning method, is also depicted in Fig. 5 for a reference. The spectrum at $\tau = 0.20$ ps shows that the L_- band rapidly disappears, while the L_+ band remains as the tail on the high-frequency side of the coherent LO phonon band. In general, this phenomenon is interpreted in terms of the relation between the decay time and phonon strength.[20,28–31] The peak frequencies of the L_+ band is slightly higher than

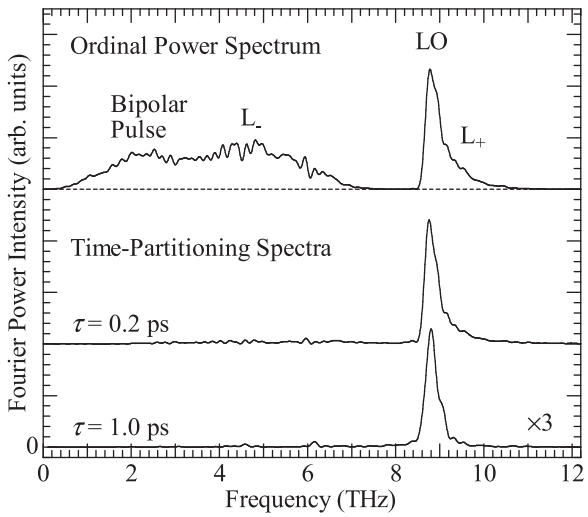

FIG. 5. Time-partitioning Fourier power spectra at $\tau = 0.2$ and 1.0 ps. For a reference, the ordinal Fourier power spectrum is depicted at on the top.

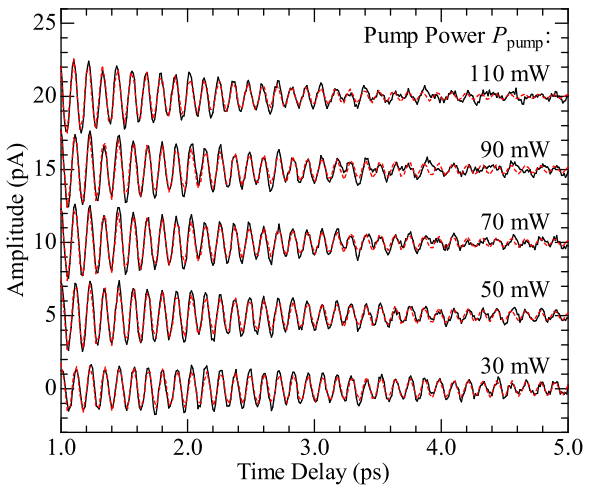

FIG. 6. (Color online) Time-domain terahertz-wave signals in the time-delay range from 1.0 to 5.0 ps. The solid and dashed lines denote the experimental data and fitting results with the use of the damped sinusoidal function, respectively.

that of the coherent LO phonon band. Accordingly, the observed L_+ mode is assigned to the LO-phonon-like mode. Meanwhile, the peak frequency of the L_- band is much lower than the frequency of the transverse optical phonon (7.98 THz). The observed L_- mode is, therefore, attributed to the plasmonlike mode. The above assignment is supported by the values of the phonon strength. The phonon-strength values of the L_+ (L_-) modes were calculated to be 0.98 (0.02) at 30 mW and 0.78 (0.22) at 110 mW, respectively, where the details of the calculation are described in APPENDIX. The phenomenological relation between the decay time and phonon strength suggests that the decay time becomes short (long) in the case that the observed mode has plasmonlike characteristics (phononlike characteristics). This is consistent with the present observation that the L_- band decays more rapidly than the L_+ band. In the spectrum at $\tau = 1.0$ ps, only the coherent LO phonon band is observed, which indicates that the coherent LO phonon signal dominates the waveforms in the time-delay range longer than ~1.0 ps shown in Fig. 3. We fitted the terahertz waveform in the above-mentioned time-domain range using a damped sinusoidal function as shown in Fig. 6. The fitted results (dashed lines) well agree with the experimental data (solid lines). The amplitude decay time obtained by the fitting is plotted as a function of pump power in Fig. 7. The decay time monotonically decreases as the pump power is increased. The decay time is 3.0 ps at the pump power of 30 mW, while the decay time is shortened to be 1.3 ps at 110 mW. Since the pump power connects with the photogenerated carrier density, the decrease of the decay time results from the scattering by the photogenerated carriers. Here, we discuss the time-delay range in which the photogenerated carriers affect the decay time of the coherent LO phonon. The bipolar pulse and coherent LOPC bands disappear in the time-partitioning Fourier power spectrum at $\tau = 1.0$ ps as shown in Fig. 5. This fact indicates that the photogenerated carriers escape from the undoped GaAs layer within 1.0 ps at least. This is an evidence that the photogenerated carriers are absent in the undoped GaAs layer in the time-delay range longer than 1.0 ps. We, therefore, conclude that the dephasing of the terahertz wave from the coherent LO phonon is dominated in the time-delay range shorter than ~1.0 ps in which the photogenerated carriers still remain in the undoped GaAs layer.

Finally, we compare the decay time of the coherent LO phonon obtained in the present work with the dephasing time of the LO phonon obtained with the use of coherent anti-Stoke Raman scattering (CARS) spectroscopy. Vallée reported that the dephasing time of the coherent GaAs LO phonon is 2.1 ps at 300 K.[32] Since the intensity of the coherent LO phonon is square of the amplitude of the coherent LO phonon, the amplitude dephasing time of the coherent LO phonon is 4.2 ps. In the CARS measurement, the excitation light is transparent to samples examined. Since the photogenerated carrier is absent, the dephasing time is determined only by the relaxation into acoustic phonon

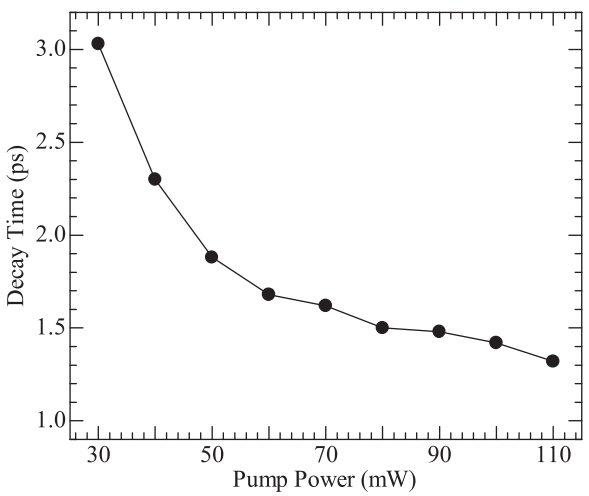

FIG. 7. Amplitude decay time (solid circle) plotted as a function of pump power. The solid line is the guide for the eye.

branches. In the present work, the amplitude decay time of the coherent phonon is 3.0 ps at the lowest pump power of 30 mW. Comparing this decay time with the amplitude dephasing time of the CARS signal (4.2 ps), we consider that the scattering effect of the photogenerated carriers is inevitable in the terahertz time-domain measurement. We also notice that the same consideration is valid in the pump-probe technique with the use of the pump light absorbed into samples. We could not observe the terahertz wave from the coherent LO phonon at the pump power lower than 30 mW. If the pump power is reduced to be of the order of a few milliwatts, we assume that the decay time of the coherent LO-phonon terahertz wave approaches 4.2 ps obtained with the use of the CARS technique because the scattering effect of the photogenerated carriers is considerably suppressed.

IV. SUMMARY

We have investigated the decay dynamics of the coherent GaAs LO phonon in the undoped GaAs/*n*-type GaAs epitaxial structure using a time-domain terahertz spectroscopic technique. We have observed the terahertz waves from the coherent LO phonon together with those from the ultrafast photocurrent and LOPC mode. The decay of the L_- mode is faster than that of the L_+ mode. We have explained the decay of the LOPC mode from the viewpoint of the relation between the decay time and phonon strength. We have found that the coherent LO phonon emits the terahertz wave up to 5.0 ps, whereas the terahertz waves from the coherent LOPC mode and from the ultrafast photocurrent disappear within 1.0 ps. The decay time of the coherent LO phonon monotonically decreases as the pump power is increased. We conclude that the dephasing of the terahertz wave from the coherent LO phonon is dominated in the time-delay range shorter than ~1.0 ps in which the photogenerated carriers remain in the undoped GaAs layer. In other words, the scattering of the photogenerated carriers within ~1.0 ps affects the dephasing of the coherent LO phonon.

ACKNOWLEDGMENTS

This work was supported by KAKENHI Grant No. 15K13341 from Japan Society for the Promotion of Science.

APPENDIX

We calculated the phonon strengths $S_{\mathrm{ph}}{}^{\mathrm{L}\pm}$ of the $L_\pm$ modes using the following equation:[31]

$$S_{\mathrm{ph}}^{\mathrm{L}_\pm} = \frac{\pm\omega_{\mathrm{L}_\pm}^2 \mp \omega_{\mathrm{p}}^2}{\omega_{\mathrm{L}_+}^2 - \omega_{\mathrm{L}_-}^2}. \tag{A1}$$

Here, ω_{L_-} and $\omega_{\mathrm{L}+}$ are the frequencies of the L_- and L_+ modes, respectively. The plasma frequency ω_{p} is given by

$$\omega_{\mathrm{p}} = \sqrt{\frac{ne^2}{\varepsilon_\infty m^*}}, \tag{A2}$$

where n is the photogenerated electron density. The quantities of m^* and ε_∞ are the electron effective mass and dielectric constant of GaAs, respectively. Equation (A1) means that the L_+ mode exhibits the phononlike characteristics with an increase in $S_{\mathrm{ph}}^{\mathrm{L}_+}$. In addition, the L_- mode becomes plasmonlike with a decrease in $S_{\mathrm{ph}}^{\mathrm{L}_+}$. We calculated the plasmon frequency using the following value: $m^* = 0.0665 m_0$ (Ref. 33) and $\varepsilon_\infty = 10.6\varepsilon_0$.[34] The quantities of m_0 and ε_0 are the free-electron mass and dielectric constant in vacuum. The average density of the photogenerated electrons n was estimated using the following equation, taking account of the fluence of the pump beam f at the sample surface, reflectance R, absorption coefficient α, and undoped GaAs layer thickness d:

$$n = \frac{f\left[1 - \exp(\alpha d)\right](1 - R)}{E_{\mathrm{ph}} d}. \tag{A3}$$

Here, E_{ph} is the photon energy of the pump beam (1.55 eV) and the values of α and R at 1.55 eV are $1.20 \times 10^4\,\mathrm{cm}^{-1}$ and 0.329, respectively.[35] The calculated plasma frequencies at the pump power of 30 and 110 mW were 3.2 and 6.2 THz, respectively. The values of ω_{L_-} ($\omega_{\mathrm{L}+}$) at 30 and 110 mW, which are obtained by the Gaussian fitting shown in Fig. 4, are 3.02 (8.89) and 5.05 (9.25) THz, respectively. Using Eqs. (A1)–(A3) together with the parameters described above, the phonon-strength values of the L_+ (L_-) modes were evaluated to be 0.98 (0.02) at 30 mW and 0.78 (0.22) at 110 mW, respectively.

[1]P. Gu and M. Tani, "Terahertz radiation from semiconductor surfaces" in *Terahertz Optoelectronics*, edited by K. Sakai (Springer, Berlin, 2005), pp. 63–97.
[2]X.-C. Zhang and D. Auston, J. Appl. Phys. **71**, 326 (1992).
[3]H. Takeuchi, J. Yanagisawa, J. Hashimoto, and M. Nakayama, J. Appl. Phys. **105**, 093539 (2009).
[4]Y. Sano *et al.*, Sci. Rep. **4**, 6046 (2014).
[5]F. R. Bagsican, I. Kawayama, H. Murakami, M. Tonouchi, A. Winchester, S. Ghosh, and S. Talapatra, e-J. Surf. Sci. Nanotechnol. **14**, 78 (2016).
[6]T. Pfiffer, T. Decorsy, W. Kütt, and H. Kurtz, Appl. Phys. A **55**, 482 (1992).
[7]A. Kuzunetson and C. Stanton, Phys. Rev. B **51**, 7555 (1995).
[8]T. Decorsy, H. Auer, H. J. Bakker, H. G. Roskos, and H. Kurz, Phys. Rev. B **53**, 4005 (1996).
[9]I. Yokota, J. Phys. Soc. Jpn. **16**, 2075 (1961).
[10]P. Gu, M. Tani, K. Sakai, and T.-R. Yang, Appl. Phys. Lett. **77**, 1798 (2000).
[11]K. Kersting, J. H. Heyman, G. Strasser, and K. Unterrainer, Phys. Rev. B **58**, 4553 (1998).
[12]M. P. Hasselbeck, D. Stalnkaer, L. A. Schile, T. J. Rotter, A. Stinz, and M. Sheik-Bahae, Phys. Rev. B **65**, 233203 (2002).
[13]Y. C. Chen, P. U. Upadhya, E. L. Linfield, H. E. Beere, and A. G. Davis, Phys. Rev. B **69**, 235325 (2004).
[14]R. Huber, F. Tauser, A. Brodschelm, M. Bicher, G. Absteiner, and A. Leitensforfer, Nature **414**, 286 (2001).
[15]R. Huber, C. Kubler, S. Tubel, A. Leitenstorfer, Q. T. Vu, H. Huang, K. Kohler, and M.-C. Amann, Phys. Rev. Lett. **94**, 027401 (2005).
[16]H. Takeuchi, T. Sumioka, and M. Nakayama, IEEE Trans. Terahertz Sci. Technol. **7**, 124 (2017).
[17]G. C. Cho, T. Decorsy, H. J. Bakker, R. Hövel, and H. Kurtz, Phys. Rev. Lett. **77**, 4062 (1996).
[18]Y. M. Chang, L. Xu, and H. W. K. Tom, Phys. Rev. Lett. **78**, 4649 (1997).
[19]M. Hase, K. Mizoguchi, H. Harima, F. Miyamaru, S. Nakashima, R. Fukasawa, M. Tani, and K. Sakai, J. Lumin. **76–77**, 68 (1998).

[20]M. Hase, S. Nakashima, K. Mizoguchi, H. Harima, and K. Sakai, Phys. Rev. B **60**, 16526 (1999).
[21]H. W. K. Tom, Y. M. Chang, and H. Kwak, Appl. Phys. B **68**, 305 (1999).
[22]K. Ishioka, M. Kitajima, and K. Ushida, J. Phys. Soc. Jpn. **75**, 084704 (2006).
[23]K. Ishioka, A. K. Basak, and H. Petek, Phys. Rev. B **84**, 235202 (2011).
[24]J. Hu, O. V. Misochiko, A. Goto, and H. Petek, Phys. Rev. B **86**, 235145 (2012).
[25]A. K. Basak, H. Petek, K. Ishioka, E. M. Tatcher, and C. J. Stanton, Phys. Rev. B **91**, 125201 (2015).
[26]H. H. Wilder, Surf. Sci. **132**, 390 (1983).
[27]D. E. Aspnes and A. A. Studna, Phys. Rev. B **7**, 4605 (1973).
[28]B. B. Varga, Phys. Rev. **137**, A1896 (1965).
[29]K. S. Singwi and M. P. Tosi, Phys. Rev. **147**, 658 (1966).
[30]F. Vallée, F. Ganikhanov, and F. Bogani, Phys. Rev. B **56**, 13141 (1997).
[31]S. Katayama, M. Hase, M. Iida, and S. Nakashima, *Proceedings of the 25th International Conference on the Physics of Semiconductors*, edited by N. Miura and T. Ando (Springer-Verlag, Berlin, 2001), p. 180.
[32]F. Vallée, Phys. Rev. B **49**, 2460 (1994).
[33]D. F. Nelson, R. C. Miller, C. W. Tu, and S. K. Sputz, Phys. Rev. B **36**, 8063 (1987).
[34]O. Madelung, *Semiconductors-Basic Data*, 2nd ed. (Springer, Berlin, 2004), p.117.
[35]D. E. Aspnes, S. M. Kelso, R. A. Logan, and R. Bhat, J. Appl. Phys. **60**, 754 (1986). The absorption coefficient and refractive index at the photon energy of 1.55 eV were derived using a linear interpolation between the values at 1.50 and 1.60 eV.